

Published in final edited form as:

*Chem Commun (Camb)*. 2009 March 21; (11): 1413–1415. doi:10.1039/b819204a.

## A novel H<sub>2</sub>O<sub>2</sub>-triggered anti-Fenton fluorescent pro-chelator excitable with visible light†

Yibin Wei and Maolin Guo\*

Department of Chemistry and Biochemistry, University of Massachusetts, Dartmouth, MA, 02747, USA

### Abstract

A chelator and a pro-chelator that can be activated by H<sub>2</sub>O<sub>2</sub> and subsequently sequesters iron and attenuates the Fenton reaction have been developed; both molecules are fluorescent excitable by visible light, and H<sub>2</sub>O<sub>2</sub>-activation, as well as iron-chelation, induces remarkable changes in fluorescence.

Abnormal accumulation of redox metals (*e.g.*, iron and copper) in certain tissues in the body and the metal-promoted Fenton reactions (eqn (1)), which yield highly reactive and deleterious oxidizing species, have been implicated in the pathogenesis of Parkinson's disease (PD), Alzheimer's disease (AD), atherosclerosis, hemochromatosis, liver damage, diabetes and cancer, *etc.*<sup>1</sup> H<sub>2</sub>O<sub>2</sub>, one of the key reactants in the Fenton reactions, is also one of the major endogenous reactive oxygen species (ROS).<sup>1</sup> H<sub>2</sub>O<sub>2</sub> is essential for cellular activities (*e.g.*, as a second messenger) but can be extremely toxic to cells at high concentrations.<sup>1</sup> The production of H<sub>2</sub>O<sub>2</sub> is significantly increased, but its elimination mechanisms become impaired, in patients with neurodegenerative disease.<sup>1d,e</sup> Elevated levels of H<sub>2</sub>O<sub>2</sub> and the Fenton reactions contribute to oxidative stress and neurodegeneration. Anti-Fenton agents offer a promise in treatment and prevention of these diseases. We and others have been developing Fenton antidotes *via* an H<sub>2</sub>O<sub>2</sub>-triggered prochelator activation and a subsequent metal caging strategy.<sup>2,3</sup> As the process involves consumption of H<sub>2</sub>O<sub>2</sub> by the prochelator, subsequent sequestration of the metal and prevention Fenton reactions, we called it an "anti-Fenton reaction".<sup>2</sup> The advantage of this strategy is that chelation can only be triggered by toxic levels of H<sub>2</sub>O<sub>2</sub> and thus will not interfere with healthy metal homeostasis. However, direct measurement of the efficacy and cellular fate of these novel compounds, currently being tested in living systems, is hindered by the lack of an easily trackable marker.



To overcome these drawbacks, we have developed our second generation prochelator, 2-boronobenzaldehyde benzoyl-hydrazone, with an anthracene fluorophore tag (**SBH-B-AN**), and the corresponding active chelator with the same tag (**SBH-AN**). Both the fluorophore-tagged prochelator and chelator give a strong fluorescent light upon excitation by UV or visible light (400 nm), thus providing an easy trace of their cellular uptake and distribution *via* a fluorescent microscope. Furthermore, the activation of the prochelator by H<sub>2</sub>O<sub>2</sub> induces a new

†Electronic supplementary information (ESI) available: Details on synthesis, absorption and fluorescence spectra and the deoxyribose assay.

© The Royal Society of Chemistry 2009

E-mail: E-mail: mguo@umassd.edu.

fluorescence peak centred at 480 nm, while the iron chelation induces a marked quenching of the fluorescence, thus allowing the anti-Fenton process to be monitored in realtime by fluorescence techniques.

**SBH-AN** and prochelator **SBH-B-AN** were synthesized by a 3-step procedure (Scheme 1 and ESI†). The iron-binding moiety salicylaldehyde benzoylhydrazone (SBH) was chosen because of its comparable iron-binding affinity to the SIH analogues,<sup>4</sup> a better lipophilicity (therefore potentially higher cell penetration) and a slower hydrolysis ( $t_{1/2}=7.9$  h) rate under physiological relevant conditions.<sup>5</sup>

First, we examined the photophysical properties of **SBH-AN** and the prochelator **SBH-B-AN** at pH 7.30. **SBH-AN** displays a spectrum similar to that of a combination of the SBH moiety and the anthracene moiety (Fig. 1(A)), assignable to the  $\pi-\pi^*$  transitions.<sup>6,7</sup> Replacing the  $-\text{OH}$  group with a boronic acid group in **SBH-B-AN** significantly changes the absorption of the SBH moiety in the UV region (270–330 nm) and the visible region (390–470 nm), while little change is observable for the anthracene moiety. Upon excitation by UV light ( $\leq 360$  nm), both compounds showed a similar photoluminescence response and give a blue fluorescence, due to the anthracene fluorophore.<sup>7</sup> Interestingly, upon excitation at 400 nm (the phenolate absorption), different emission profiles were observed: the prochelator **SBH-B-AN** showed a single fluorescence band at 440 nm while the active chelator **SBH-AN** displayed a strong additional fluorescence band at  $\sim 480$  nm (Fig. 1(B)). This characteristic allows for realtime fluorescent monitoring the response of **SBH-B-AN** to  $\text{H}_2\text{O}_2$ .

Second, we examined the spectroscopic changes when prochelator **SBH-B-AN** reacted with  $\text{H}_2\text{O}_2$ . Upon adding  $\text{H}_2\text{O}_2$  to **SBH-B-AN** in DMF (*N,N*-dimethylformide)–KPB (potassium phosphate buffer) (20 mM, pH 7.3, v/v, 1 : 1), no change occurred to the fluorescence peak at 440 nm, while a new peak emerged at 480 nm and grew over time (Fig. 2(A)). The final fluorescence spectrum of the mixture almost matches that of **SBH-AN**, implying a conversion of **SBH-B-AN** to **SBH-AN**. A 5.5-fold increase in intensity at 520 nm was observed.

To further characterize the chemistry of the conversion, the reaction was followed by  $^1\text{H}$  NMR in dimethylsulfoxide (DMSO). After incubating **SBH-B-AN** with  $\text{H}_2\text{O}_2$ ,  $^1\text{H}$  NMR peaks (Fig. S1†) for **SBH-B-AN** ( $\delta 11.05(\text{s})$ ,  $-\text{NH}-$ ;  $\delta 8.76(\text{s})$ ,  $-\text{CH}=\text{N}-$ ;  $\delta 8.50(\text{s})$ ,  $-\text{B}(\text{OH})_2$ ) gradually decreased in intensity, while the peaks corresponding to **SBH-AN** ( $\delta 12.08(\text{s})$   $-\text{NH}-$ ;  $11.30(\text{s})$ ,  $-\text{OH}-$ ;  $8.64(\text{s})$ ,  $-\text{CH}=\text{N}-$ ) appeared simultaneously and increased in intensity with time. The peaks ( $\delta 7.44-7.37(\text{m})$ ,  $7.30(\text{t})$  and  $6.95-6.90(\text{m})$ , salicyl-aldehyde) also underwent similar conversions. Meanwhile, the peak for boric acid, the deprotection product of boronic acid by  $\text{H}_2\text{O}_2$ , appeared at  $\delta 6.55(\text{s})$ . No  $^1\text{H}$  NMR change was observed for the anthracene moiety due to its distance from the reaction site. In  $\sim 4$  h, **SBH-B-AN** had been cleanly converted to **SBH-AN** with no intermediate formed, as indicated by the  $^1\text{H}$  NMR spectra. The conversion from **SBH-B-AN** to **SBH-AN** was also confirmed by UV-vis difference spectra in DMF–KPB (20 mM, pH 7.3, v/v, 1 : 1) (Fig. S2†). With a ten-fold excess of  $\text{H}_2\text{O}_2$ , the conversion reaction is pseudo-first order with an apparent rate constant ( $K_{\text{obs}}$ ) of  $4.37 \times 10^{-4} \text{ s}^{-1}$ .

Third, we investigated whether **SBH-AN** and **SBH-B-AN** bind iron under physiological relevant conditions and whether the chelation can be detected by fluorescent techniques. Since metal binding to SBH induces characteristic changes to the absorption bands,<sup>6,8</sup> UV-vis titration was performed first to probe the binding between **SBH-AN** and  $\text{Fe}^{\text{III}}$  in potassium phosphate buffer (KPB), pH 7.30. Although the changes in spectra were largely obstructed by the strong absorption from the anthracene moiety in the UV region, evident spectroscopic changes due to iron-binding were observed (Fig. S3†): a decrease in intensity around 330 nm with simultaneous increases in intensity around 370 nm and in the visible region (400–500 nm). These changes match those reported for  $\text{Fe}$ –SBH complexation,<sup>8</sup> suggesting the

formation of specific **SBH-AN**-Fe complexes. However, when a similar titration was performed with the pro-chelator, no change in absorption was observed in the UV-vis region (Fig. S4†), indicating no interaction between the pro-chelator with Fe<sup>III</sup> under the conditions applied. However, upon the addition of H<sub>2</sub>O<sub>2</sub> to the mixture, characteristic absorption bands for Fe-binding emerged and increased in intensity (Fig. S5†), suggesting the formation of **SBH-AN**-Fe complexes. The spectroscopic changes indicate that H<sub>2</sub>O<sub>2</sub> “activates” **SBH-B-AN** to **SBH-AN**, which subsequently chelates iron (Fig. S6†). Interestingly, iron-binding also induces marked fluorescent changes. Titration of the chelator **SBH-AN** with Fe<sup>III</sup> induced a quenching of fluorescence for both the 440 nm and 480 nm bands (Fig. 2(B)), presumably due to metal-coordination-induced molecular collisional quenching. In contrast, similar titration experiments with the prochelator **SBH-B-AN** induced little fluorescent change (Fig. S7†).

Finally, we tested the anti-Fenton activities of **SBH-AN** and **SBH-B-AN** using a 2-deoxyribose degradation assay.<sup>2</sup> As shown in Fig. 3, both **SBH-B-AN** and **SBH-AN** at a 2 : 1 chelator :Fe ratio significantly inhibited hydroxyl radical-induced 2-deoxyribose degradation, indicating that **SBH-B-AN** and **SBH-AN** efficiently attenuate the Fenton reaction under physiologically relevant conditions.

In summary, we have developed a novel fluorescent pro-chelator, **SBH-B-AN**, and an active chelator **SBH-AN**, both excitable by non-damaging visible light. **SBH-B-AN** can sense H<sub>2</sub>O<sub>2</sub> and be converted to **SBH-AN**, which subsequently sequesters iron and attenuates the Fenton reaction. The H<sub>2</sub>O<sub>2</sub>-activation and the iron-chelation processes produce specific fluorescent changes. These novel properties may be utilized in the realtime monitoring of cellular oxidative stress status (H<sub>2</sub>O<sub>2</sub> levels) and in tracking their anti-Fenton efficacy and metabolism in living systems by fluorescent techniques.

## Supplementary Material

Refer to Web version on PubMed Central for supplementary material.

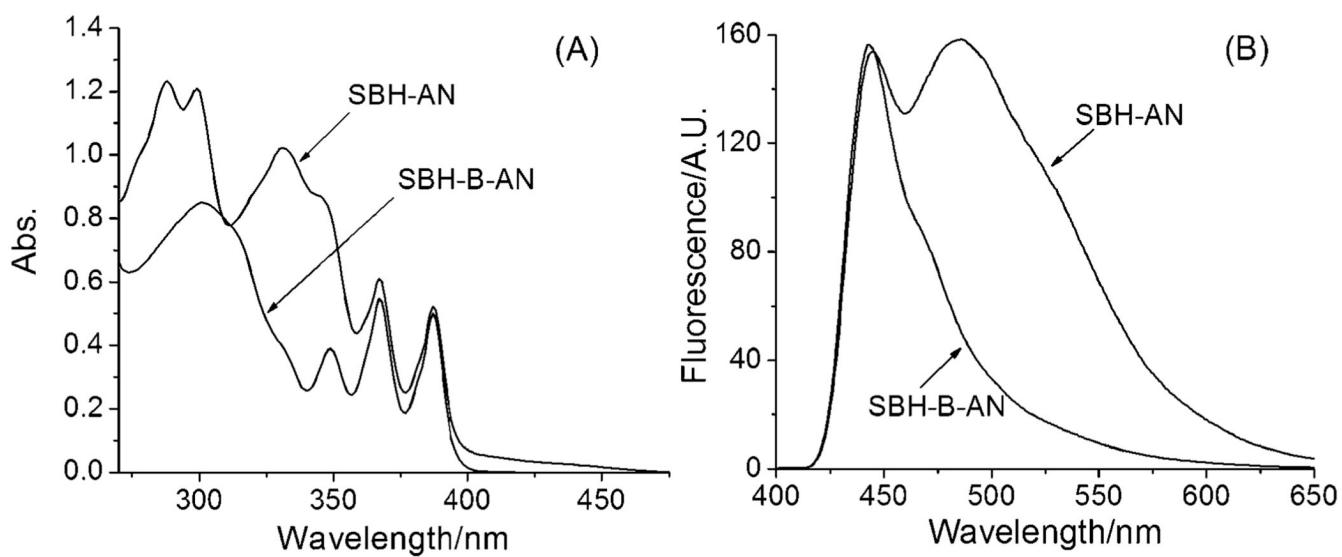
## Acknowledgments

Acknowledgement is made to the University of Massachusetts, Dartmouth, the American Parkinson Disease Association, National Parkinson Foundation and the National Institutes of Health for funding. This publication was made possible by Grant Number 1 R21 AT002743-02 from the National Center for Complementary and Alternative Medicine (NCCAM). Its contents are solely the responsibility of the authors and do not necessarily represent the official views of the NCCAM, or the National Institutes of Health.

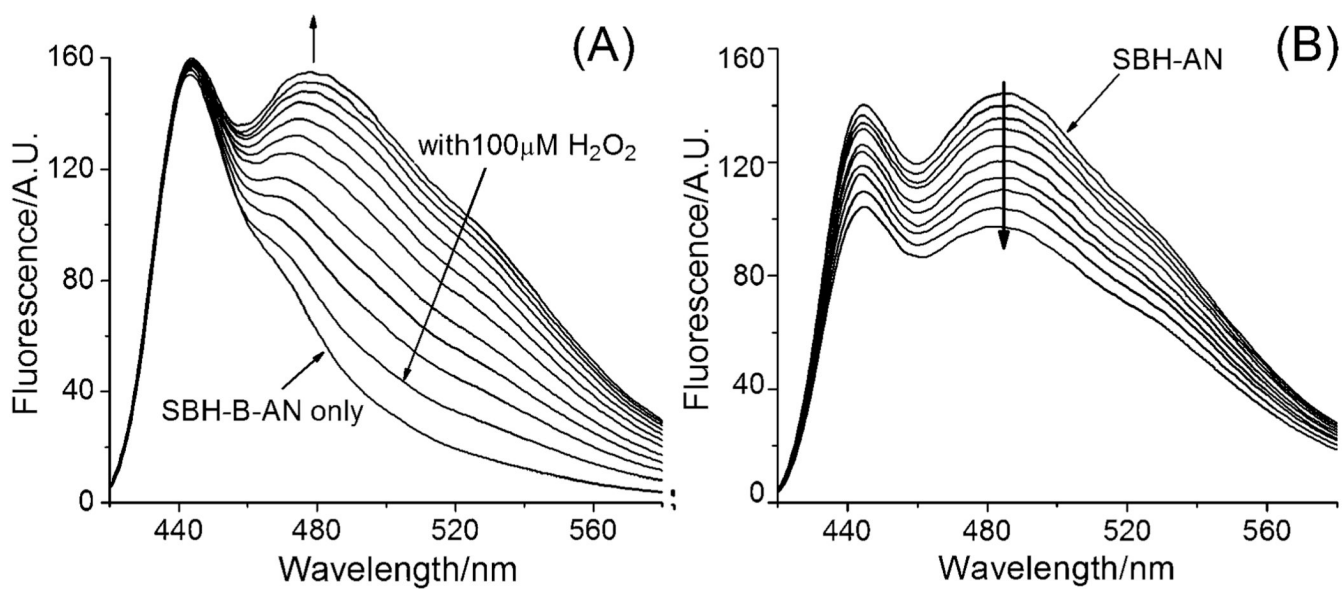
## Notes and references

1. Crichton, R. *Inorganic Biochemistry of Iron Metabolism*. West Sussex: John Wiley & Sons, Ltd; 2001. (b) Barnham KJ, Masters CL, Bush AI. *Nat. Rev. Drug Discovery* 2004;3:205–214. (c) Perez CA, Tong Y, Guo M. *Curr. Bioactive Comp* 2008;4:150–158. (d) Krapfenbauer K, Engidawork E, Cairns N, Fountoulakis M, Lubec G. *Brain Res* 2003;967:152–160. [PubMed: 12650976] (e) Tabner BJ, Turnbull S, El-Agnaf OMA, Allsop D. *Free Radical Biol. Med* 2002;32:1076–1083. [PubMed: 12031892]
2. Wei Y, Guo M. *Angew. Chem., Int. Ed* 2007;46:4722–4725.
3. Charkoudian LK, Pham DM, Franz KJ. *J. Am. Chem. Soc* 2006;128:12424–12425. [PubMed: 16984186]
4. Chaston TB, Richardson DR. *Am. J. Hematol* 2003;73:200–210. [PubMed: 12827659]
5. Buss JL, Neuzil J, Gellert N, Weber C, Ponka P. *Biochem. Pharmacol* 2003;65:161–172. [PubMed: 12504792]
6. Lu Y-H, Lu Y-W, Wu C-L, Shao Q, Chen X-L, Bimbong RNB. *Spectrochim. Acta, Part A* 2006;65:695–701.

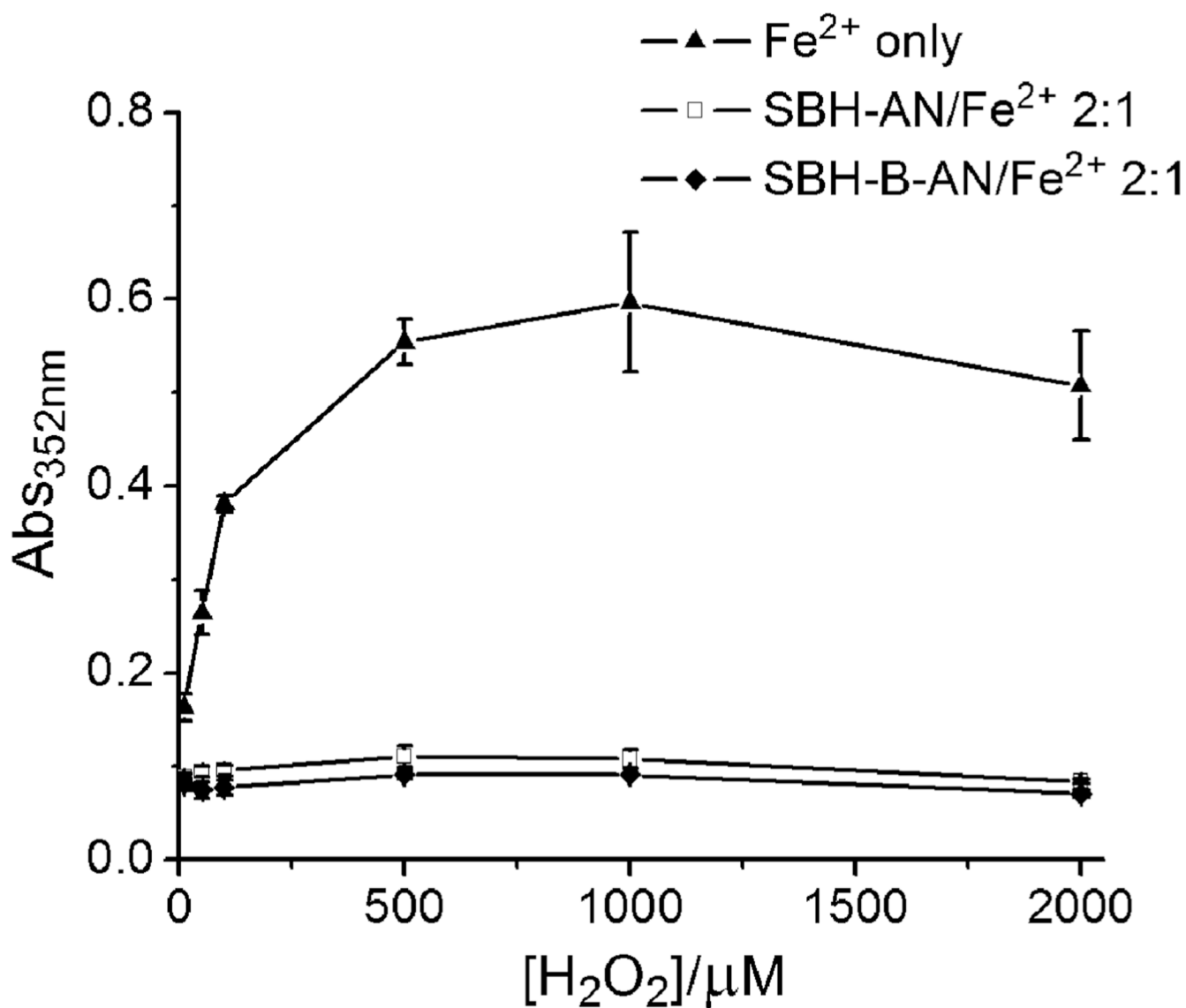
7. Nakajima A. *J. Lumin* 1977;15:277–282.
8. Dubois JE, Fakhrayan H, Doucet JP, El Hage Chahine JM. *Inorg. Chem* 1992;31:853–859.



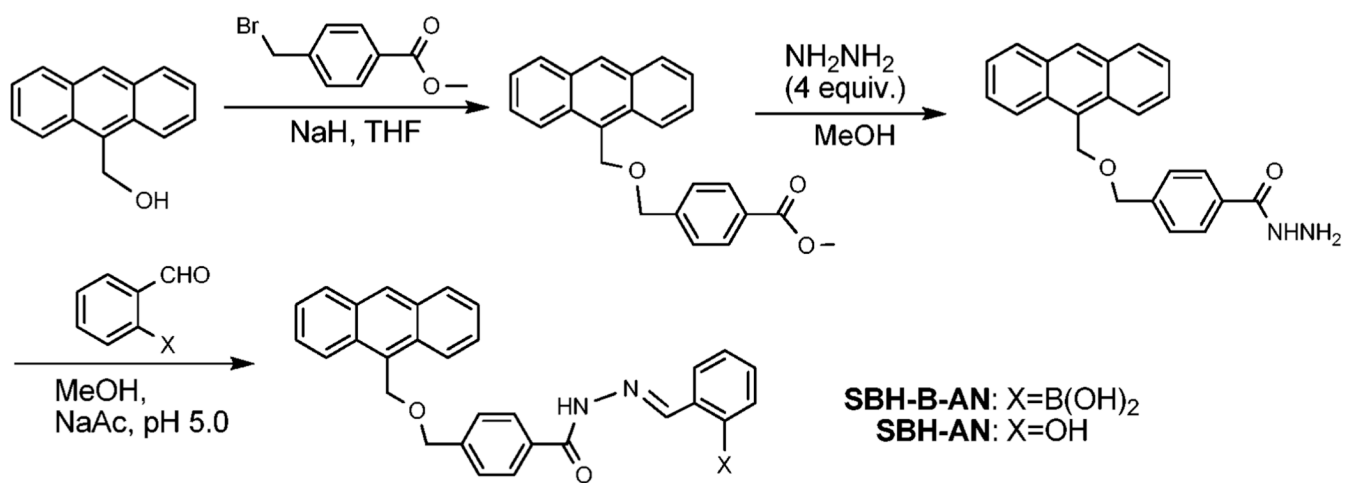
**Fig. 1.** (A) UV-vis spectra and (B) fluorescence spectra ( $\lambda_{\text{ex}} = 400$  nm, with a 415 nm cutoff filter) of 10  $\mu\text{M}$  **SBH-B-AN** and **SBH-AN** in DMF/KPB (1 : 1), pH 7.30, at 298 K.



**Fig. 2.** (A) Fluorescence spectra ( $\lambda_{\text{ex}} = 400$  nm) of the time course of the reactions of 10  $\mu\text{M}$  **SBH-B-AN** with 100  $\mu\text{M}$   $\text{H}_2\text{O}_2$  (0 to 120 min); (B) fluorescence ( $\lambda_{\text{ex}} = 400$  nm) titration of 10  $\mu\text{M}$  **SBH-AN** with  $\text{Fe}^{\text{III}}$  in 1  $\mu\text{M}$  increments in DMF-KPB (1 : 1), pH 7.30, at 298 K.



**Fig. 3.** Effect of **SBH-AN** and **SBH-B-AN** on the oxidative degradation of 2-deoxyribose promoted by  $\text{Fe}^{\text{II}}$  ( $20 \mu\text{M}$ ) in the presence of  $\text{H}_2\text{O}_2$  and hydroascorbate ( $5 \text{ mM}$ ) in  $20 \text{ mM}$  KPB, pH 7.20.



**Scheme 1.**  
Synthesis and abbreviations of the compounds.